

s), 2.18 (3 H, s), 2.22 (3 H, s), 2.64 (2 H, m), 3.58 (1 H, d, $J = 11.8$ Hz), 3.67 (1 H, d, $J = 11.8$ Hz), 4.69 (2 H, s), 7.29-7.53 (5 H, m); IR (liquid film) 3240 (br), 1265 (s), 1130 (s), 1040 (s), 910 (s), 870 (s), 815 (s), 715 (s), 700 (s) cm^{-1} . (S)-(-)-MTPA ester derivative of (S)-**8**: ^1H NMR (CDCl_3) δ 1.1-1.9 (4 H, m), 2.04 (3 H, s), 2.15 (3 H, s), 2.20 (3 H, s), 2.60 (2 H, m), 3.56 (3 H, q, $J = 1.1$ Hz), 4.28 (1 H, d, $J = 11.2$ Hz), 4.41 (1 H, d, $J = 11.2$ Hz), 4.68 (2 H, s), 7.29-7.60 (10 H, m). (S)-(-)-MTPA ester derivative of (\pm)-**8**:²⁷ ^1H NMR (CDCl_3) δ 1.1-1.9 (4 H, m), 2.01 (3 H, s), 2.04 (3 H, s), 2.15 (3 H, s), 2.20 (3 H, s), 2.60 (2 H, m), 3.55 (3 H, q, $J = 1.1$ Hz), 3.56 (3 H, q, $J = 1.1$ Hz), 4.26 (1 H, d, $J = 11.2$ Hz), 4.28 (1 H, d, $J = 11.2$ Hz), 4.41 (1 H, d, $J = 11.2$ Hz), 4.47 (1 H, d, $J = 11.2$ Hz), 4.68 (2 H, s), 7.29-7.60 (10 H, m).

8 (18.7 mg, 0.0574 mmol) was oxidized by Collins reagent as described by Cohen et al.^{15b} to give 14.7 mg (79%) of the chroman aldehyde: $[\alpha]_{\text{D}}^{25}$ 12.3 (c 0.323, CHCl_3), lit. $[\alpha]_{\text{D}}^{20}$ 12.5 (c 2.8, CHCl_3),^{17d} the

^1H NMR spectrum of this aldehyde was identical with their reported values.^{15b}

Acknowledgment. This work was supported partially by Grant-In-Aid for Scientific Research from the Japan Ministry of Education, Science and Culture (No. 61750821).

Supplementary Material Available: Reaction of **2a-eq** with $\text{Et}_3\text{SiH-TiCl}_4$ and the conversion of the product **6** to (*R*)-2-phenylpropanol; preparation of **10** and **11**; ^1H NMR, IR, mass and high resolution mass spectral data of **2a-eq**, **2a-ax**, **2c-eq**, **2c-ax**, **2d**, and **3a-e**; ^1H NMR spectral data of **3f**, **3g**, and the MTPA esters of **5a-f** (10 pages). Ordering information is given on any current masthead page.

Studies on the Radical Species of 9-Decarboxymethoxatin

Evelyn J. Rodriguez,[†] Thomas C. Bruice,*[†] and Dale E. Edmondson[†]

Contribution from the Department of Chemistry, University of California at Santa Barbara, Santa Barbara, California 93106, and the Department of Biochemistry, Emory University School of Medicine, Atlanta, Georgia 30322. Received July 16, 1986

Abstract: Spectrophotometric titrations have been employed to determine the pK_a values of the acid-base species of 9-decarboxymethoxatin ($\text{A} = \text{I}_{\text{ox}}\text{H}_3^+ + \text{I}_{\text{ox}}\text{H}_2 + \text{I}_{\text{ox}}\text{H}^- + \text{I}_{\text{ox}}^{2-}$; eq 1) and its quinol 2e⁻ reduction product ($\text{B} = \text{I}_{\text{red}}\text{H}_4 + \text{I}_{\text{red}}\text{H}_3^- + \text{I}_{\text{red}}\text{H}_2^{2-} + \text{I}_{\text{red}}\text{H}^{3-} + \text{I}_{\text{red}}^{4-}$; eq 3) as well as the equilibrium constants for the pH-dependent hydration of 9-decarboxymethoxatin (to provide the species $\text{C} = \text{I}_{\text{ox}}(\text{OH})^{3-} + \text{I}_{\text{ox}}(\text{H}_3\text{O})^{2-}$; eq 4). The pH dependence of the concentrations of paramagnetic semiquinone species present in solutions of half-reduced methoxatin at basic pH values ($\text{D} = \text{I}_{\text{rad}}\text{H}^{2-} + \text{I}_{\text{rad}}^{3-}$) was determined by EPR measurements, and from these concentrations the pH-dependent equilibrium constants (K_{pH}) were calculated for disproportionation of quinone and quinol species. A plot of $\log K_{\text{pH}}$ vs. pH was found to have a bell shape with ascending and descending legs of slope +1 and -1, respectively. The experimental points of the $\log K_{\text{pH}}$ vs. pH profile were fitted by an equation which takes into account the pH dependence of the concentrations of all quinone, quinol, and semiquinone species ($K_{\text{eq}} = [\text{D}]^2/[\text{A} + \text{C}][\text{B}]$). Fitting of the equation to the experimental points was carried out by iteration of the value of $K = [\text{I}_{\text{rad}}^{2-}]/[\text{I}_{\text{ox}}^{2-}][\text{I}_{\text{red}}\text{H}_2^{2-}] = 3.3$ and the pK_a of the semiquinone ($\text{I}_{\text{rad}}\text{H}^{2-}$) hydroxyl proton as 7.52. The sharp decrease in semiquinone formation above pH 12.5 is explained by quinone hydration. Spectral evidence is presented which supports the dimerization in aqueous solution of the paramagnetic semiquinone to a diamagnetic species. Analysis of the EPR spectrum of $\text{I}_{\text{rad}}^{3-}$ and comparison to the EPR spectrum of the analogous methoxatin semiquinone shows that there are no major alterations in spin density in the heterocyclic trinuclear ring system on replacement of the 9-position carboxylate functionality in the naturally occurring methoxatin with a proton.

The compound 4,5-dihydro-4,5-dioxo-1*H*-pyrrolo[2,3-*f*]quinoline-2,4,9-tricarboxylic acid (trivial name methoxatin) was first recognized to be a cofactor in methyltrophic bacteria (1979).¹



For these aerobic organisms, methoxatin-containing enzymes (quinoenzymes) serve in place of the nicotinamide cofactor requiring enzymes and flavoenzymes in the oxidation of alcohols, hexoses, aldehydes, and methylamine.² More recently, methoxatin has been found³ as a cofactor in *E. coli*, an aerobic organism, and to (most likely) represent the long sought-after cofactor for mammalian plasma amine oxidase.⁴ Quinoenzymes would appear, therefore, to represent a new and widely distributed class of oxidase enzymes.

Knowledge of the chemistry of a methoxatin semiquinone species is important to an understanding of the biological role of methoxatin. In the metabolism of methyltrophs, methoxatin is proposed to undergo 2e⁻ reduction by substrate and to pass on 1e⁻ at a time to cytochrome *c*^{5a} via ubiquinone.^{5b} Such a 2e⁻-to-1e⁻ switching mechanism must involve a methoxatin radical intermediate. Step-down electron switching mechanisms have previously been associated with a number of flavoenzymes (e.g., succinic acid dehydrogenase).⁶ The mechanisms of 2e⁻ oxidations of substrates by methoxatin and quinoenzymes are poorly understood, and as is the case with flavin and flavoenzyme oxidations,

(1) Salisbury, S. A.; Forrest, H. S.; Cruse, W. B. T.; Kennard, O. *Nature (London)* **1979**, *281*, 843.

(2) Duine, J. A.; Frank, J., Jr. *Trends Biochem. Sci. (Pers. Ed.)* **1981**, *6*(10), 278.

(3) (a) Hommes, R. W. J.; Postma, P. W.; Neijssel, O. M.; Tempest, D. W.; Dokter, P.; Duine, J. A., *FEMS Microbiol. Lett.* **1984**, *24*, 329. (b) Ameyama, M.; Shinagawa, E.; Matsushita, K.; Adachi, O. *Agric. Biol. Chem.* **1984**, *12*, 3099. (c) Ameyama, M.; Nanobe, E. S.; Matsushita, K.; Takimoto, K.; Adachi, O. *Agric. Biol. Chem.* **1986**, *50*(1), 49.

(4) Lobenstein-Verbeek, C. L.; Jongejan, J. A.; Frank, J.; Duine, J. A. *FEBS Lett.* **1984**, *170*, 305.

(5) (a) Duine, J. A.; Frank, J.; DeRuiter, L. G. *J. Gen. Microbiol.* **1979**, *115*, 523-526. (b) Beardmore-Gray, M.; Anthony, G. *J. Gen. Microbiol.* **1986**, *132*, 1257.

(6) Walsh, C. *Enzymatic Reaction Mechanism*; W. H. Freeman: San Francisco, 1970; p 377.

[†]University of California at Santa Barbara.

[†]Emory University School of Medicine.

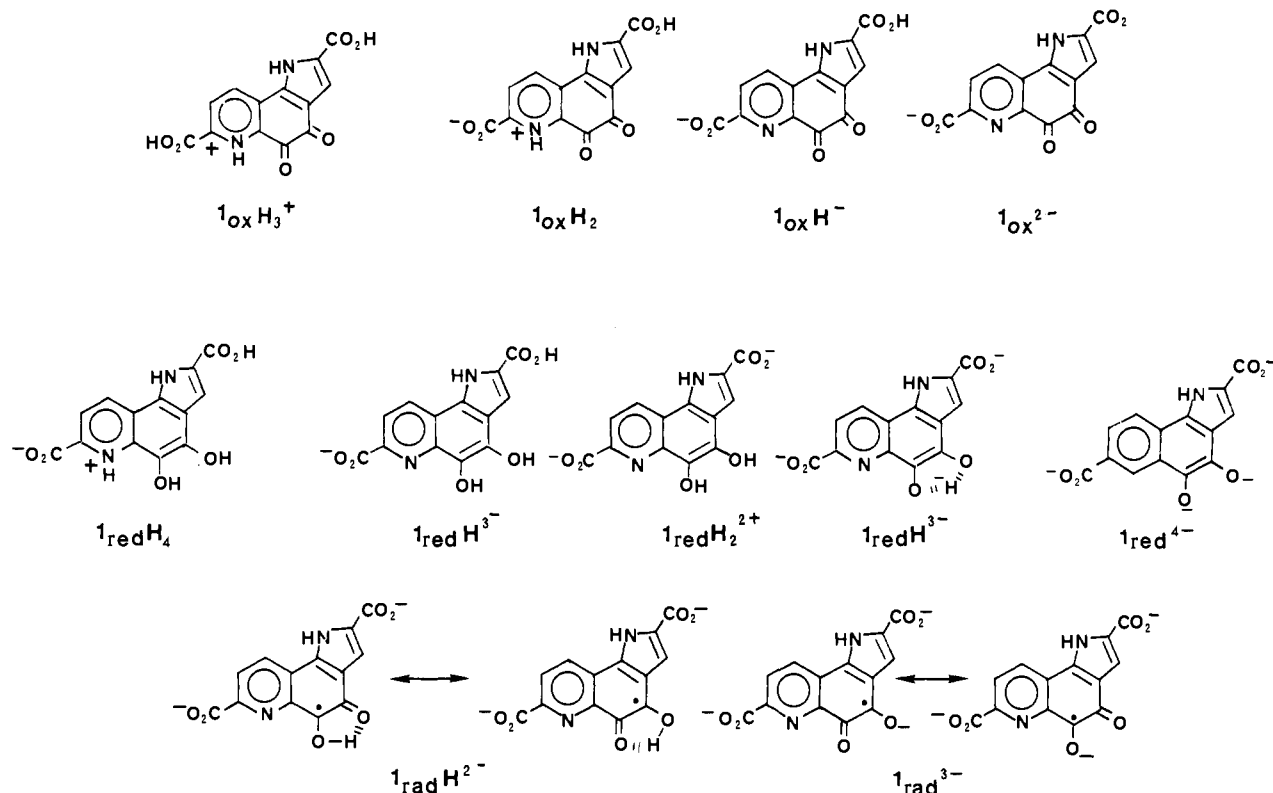


Figure 1. Structures of 9-decarboxymethoxatin and its $2e^-$ and $1e^-$ reduction products.

they may in cases represent sequential $1e^-$ transfers with radical intermediates. Methanol dehydrogenase E.C. 1.199.8 contains two methoxatin molecules,⁷ and an appreciable fraction of the cofactor can exist in the semiquinone form. The semiquinone species has been proposed to arise by comproportionation of enzyme-bound oxidized and reduced cofactor molecules. Only the enzyme species with both methoxatin cofactor molecules fully oxidized possesses catalytic activity.⁸ The semiquinone of methoxatin has been proposed as an intermediate in the inactivation of a quinoenzyme by suicide substrates.⁹

The present study represents an investigation of the solution properties of 9-decarboxymethoxatin and its $2e^-$ reduction product, as well as the pH dependence of the comproportionation of oxidized and reduced forms to provide semiquinone and the EPR and UV/vis characterization of this species. Structures and abbreviations are provided in Figure 1. All pK_a values provided in the text are macroscopic. The assignments of the structures to $1_{ox}H_2$ and $1_{red}H_4$ are based upon results with similar systems. In this laboratory we have been investigating the mechanisms of oxidations with quinoquinones and related quinones and the dependence of chemical properties on substituents.^{11,12} 9-Decarboxymethoxatin (9DCM, 1_{ox}) has been employed in this study.

Experimental Section

Instruments. Ultraviolet and visible absorbance data were recorded on Cary Models 118C and 15 spectrophotometers. Measurements of pH were performed by using either a doubly standardized Radiometer 26 or a Beckman 4500 digital pH meter. Values of pD in D_2O were deter-

mined by applying a correction of 0.16 to the pH meter reading. EPR measurements were performed by using either a Varian E4 or an IBM/Bruker ER 220 instrument. EPR spectral simulations were performed on an Aspect 2000 computer using standard Bruker software. Gaussian line shapes were employed with a line width of 0.1 G.

Acid-Base Titration. The acid-base dissociation constants for $1_{ox}H_2$ and $1_{red}H_2^{2+}$ were determined at 30 °C by spectrophotometric titration. In a typical experiment, a 1 M KCl solution was adjusted to the starting pH and was made anaerobic by at least eight cycles of alternating vacuum and flushing with argon that had been purified from any residual oxygen by passage through an OxyClear cylinder. Stock diol solution (50 μ L, 6×10^{-4} M) and an excess amount of sodium dithionite were then added under an argon stream. Similarly, the base solutions used for the titration were degassed by consecutive freeze-pump-thaw cycles. Formation of the pseudobase of 1_{ox}^{2-} was monitored by spectrophotometric titration at 30 °C with $\mu = 1.0$ (NaClO₄, 1 M).

EPR Measurements. Samples were diluted from a stock Me₂SO solution (2.6 mM) 1:10 v/v in various aqueous buffers ($\mu = 0.1$) at various pH values. All buffers were treated with Chelex to remove any trace metal contaminants. Aqueous solutions of 1_{ox} were placed in a glass side-arm assembly attached to a quartz EPR flat cell, degassed by at least six cycles of vacuum, flushed with highly purified argon, and half-reduced with a standardized solution of Na₂S₂O₄. The half-reduced solution was then transferred into the flat cell and the EPR spectrum measured at ambient temperature. Overmodulated spectra (modulation amplitude of 2 G) were used for spectra used in quantitation of the concentrations of 1_{rad}^{3-} . Double integrations were performed using a diphenylpicrazyl-hydrazide solution in toluene as a standard. Modulation amplitudes of 0.05–0.1 G were used in measuring high-resolution spectra. A microwave power level of 1 mW was used in all spectra and shown not to be saturating.

Semiquinone Visible Spectrum. Under a N₂ atmosphere, degassed buffered solutions of 1_{oxT} (5.47×10^{-4} M) and 1_{redT} (2.3×10^{-4} M) were placed in the separate compartments of two tandem cuvettes. By use of a Cary 118 spectrophotometer, one cuvette was, without mixing, placed in the reference compartment and, after mixing, the other cuvette was placed in the sample compartment. The differential spectrum was recorded from 500 to 350 nm.

Results and Discussion

Aqueous Acid-Base Chemistry. The pK_a values used in eq 1 were calculated by monitoring the absorbance change at 315 and 275 nm at 30 °C from $H_0 = -4.4$ to pH 4.29. As expected, the addition of a carboxyl group to the 7-position decreases the electron

(7) Duine, J. A.; Frank, J. J.; Verwiel, E. F. *Eur. J. Biochem.* **1981**, *118*, 395–399.

(8) Duine, J. A.; Frank, J. In *Microbial Growth on C₁ Compounds*; Dalton, H., Ed.; Heyden: London, 1981; pp 37–41.

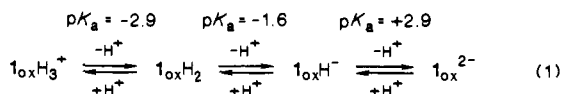
(9) Dijkstra, M.; Frank, J.; Jongejan, J. A.; Duine, J. A. *Eur. J. Biochem.* **1984**, *140*, 369–373.

(10) Noar, J. B.; Rodriguez, E. J.; Bruce, T. C. *J. Am. Chem. Soc.* **1985**, *107*, 7198.

(11) Sleath, P. R.; Noar, J. B.; Eberlein, G. A.; Bruce, T. C. *J. Am. Chem. Soc.* **1985**, *107*, 3328.

(12) (a) Eckert, T. S.; Bruce, T. C. *J. Am. Chem. Soc.* **1983**, *105*, 4431.

(b) Dekker, R. H.; Duine, J. A.; Frank, J.; Verwiel, E. J.; Westerling, J. *Eur. J. Biochem.* **1982**, *125*, 69.

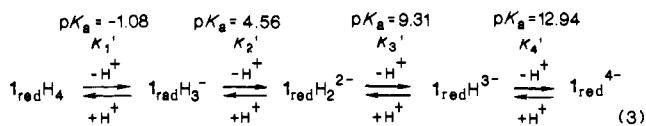


density in the pyridine ring considerably, and this is reflected in the lowering of the pK_a of the pyridinium ion in 9-decarboxymethoxatin compared to that of 7,9-didecarboxymethoxatin ($pK_a = 1.41$). The carboxyl group in the pyrrole ring is less affected by this perturbation, and this is reflected in the lowering of the pK_a of only 0.3 in 9-decarboxymethoxatin as compared to 7,9-didecarboxymethoxatin. The UV/vis spectrum of 1_{ox} is compared to that of methoxatin and 7,9-didecarboxymethoxatin in Figure 2. Inspection of Figure 2 and its caption reveals that the absence of the 7- and/or 9-carboxyl groups alters the electronic spectrum of methoxatin. Of the three absorbance maxima for methoxatin (248, 274, and 329), the long-wavelength absorbance exhibits a 10-nm hypsochromic shift for the removal of each carboxyl group (methoxatin \rightarrow 9-decarboxymethoxatin \rightarrow 7,9-didecarboxymethoxatin), while the extinction coefficients for this absorbance are insensitive to carboxyl anion substitution. The intermediate absorbance of methoxatin exhibits a marked increase in extinction coefficient in each of the stepwise removals with a very small hypsochromic shift, while the short-wavelength λ_{max} of methoxatin decreases in extinction on stepwise removal of the carboxylate group. Changes in electronic transitions with substitution must be reflected to some extent in the chemical properties of the quinone. However, it should be noted that the electron transfer potentials of methoxatin are not altered by removal of both 7- and 9-carboxyls.¹¹

The pK_a values for $1_{red}H_3^-$, $1_{red}H_2^{2-}$, and $1_{red}H^{3-}$ were determined spectrophotometrically under anaerobic conditions by monitoring the change in absorbance as a function of pH. The first spectral titration was carried out between pH 0 and 2 by monitoring the decrease in absorbance at 394 and 314 nm. A pK_a below pH 0 was determined by use of eq 2. The log of the

$$\begin{aligned}
 \Delta Abs &= \frac{a_H}{a_H + K_a} \\
 \Delta Abs(a_H + K_a) &= a_H \\
 \Delta Abs &= 1/K_a(a_H(1 - Abs)) \quad (2)
 \end{aligned}$$

slope of plots of the absorbance (Abs) vs. $a_H(1 - Abs)$ gave a $pK_a = -1.08 \pm 0.04$ (two determinations). An increase of the pH from 3 to 7 resulted in an observed decrease in absorbance at 313 and 380 nm with isosbestic points at 360 and 330 nm. Plots of A_{313} and A_{380} vs. pH fit titration curves for the dissociation of a single proton, allowing the calculation of a pK_a of 4.56 ± 0.3 by least-squares analysis. In like fashion, pK_a values of 9.31 and 12.94 were calculated for single proton dissociations from the decrease in A_{296} on increasing the pH from 7 to 11 and from the decrease in A_{312} on increasing the pH from 11 to 13.5 (eq 3). The pK_a



values obtained from $1_{red}H_2^{2-}$ and $1_{red}H^{3-}$ compare favorably with those of catechol (9.2 and 13).¹³ It should be noted that the pK_a for $1_{red}H_2^{2-}$ is almost 0.8 higher than that for the reduced form of 7,9-didecarboxymethoxatin ($pK_a = 8.54$).

It is known that *o*-quinones such as methoxatin are hydrated at high pH values.¹² Spectral changes were monitored on titration of 1_{ox}^{2-} from pH 8 to 13. Below pH 12.4 shifts were observed in λ_{max} values from 275 to 285 nm and from 315 to 340 nm with isosbestic points at 278, 304, and 328 nm. Above pH 12.4 the λ_{max} values shift from 285 to 273 nm and from 340 to 335 nm.

(13) *Critical Stability Constants*; Martell, A. E.; Smith, R. M., Eds.; Plenum: New York, 1977.

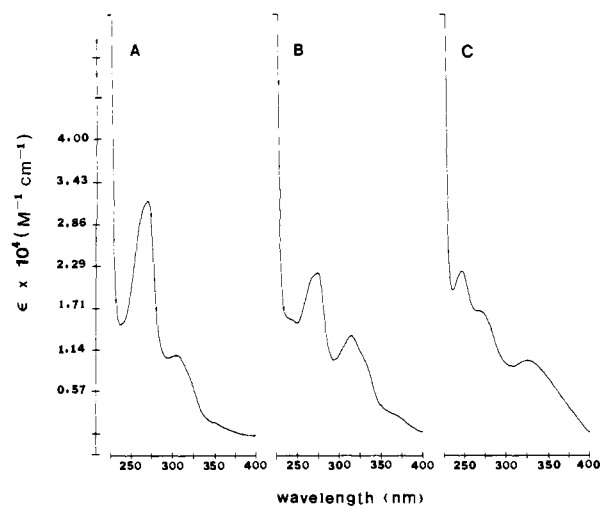
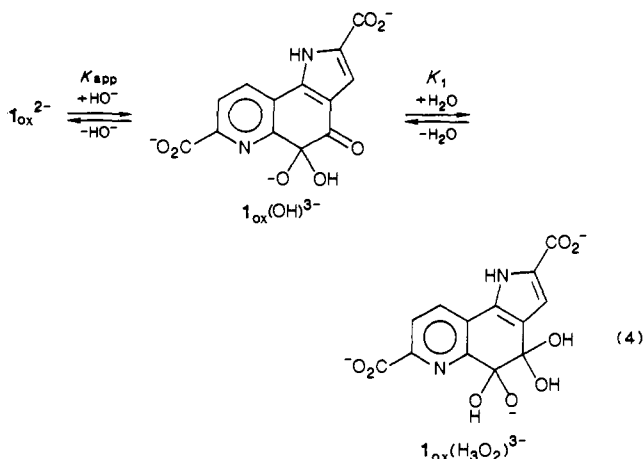


Figure 2. Absorption spectra of 7,9-didecarboxymethoxatin (A), 9-decarboxymethoxatin (B), and methoxatin (C). Spectra taken in aqueous solution at pH 7.00 buffered with potassium phosphate ($\mu = 0.1$): (A) λ_{max} 271 ($\epsilon 3.1 \times 10^4 M^{-1} cm^{-1}$), 306 ($\epsilon 1.03 \times 10^4$); (B) λ_{max} 276 ($\epsilon 2.2 \times 10^4$), 316 ($\epsilon 1.36 \times 10^4$); (C) λ_{max} 248 ($\epsilon 2.15 \times 10^4$), 274 ($\epsilon 1.6 \times 10^4$), 329 ($\epsilon 9.9 \times 10^3$).

The proton dissociation observed below pH 12.4 may be attributed to a covalent hydration equilibria as described by eq 4. Least-



squares data analysis of titration curves for the changes in absorbance at several wavelengths yielded a $pK_{app} = 10.73 \pm 0.3$. The titration curves can be described¹² by eq 5 so that $K_{app}(1 + K_1)$ may be calculated to be $1.27 \times 10^3 M^{-1}$. This value may

$$\Delta A = \frac{a_H}{K_w K_{app}(1 + K_1) + a_H} \quad (5)$$

be compared to values of $4.82 \times 10^3 M^{-1}$ obtained for 7,9-didecarboxymethoxatin and $5.50 \times 10^3 M^{-1}$ for 4,7-phenanthroline-5,6-quinone.¹¹ The spectral changes above pH 12.4 could be attributed, a priori, to either ionization of the pyrrole proton or to contraction of the hydrated anionic quinone ring. It is known that *o*-quinones may undergo ring contraction at very high pH values.¹¹ The latter was proven not to be the case with 9-decarboxymethoxatin. Thus, when the quinone was dissolved in a strongly basic solution and stored for 18 h at 30 °C, adjustment to pH 4 regenerated the quinone spectrum.

Semiquinone Formation. Below pH 9 no EPR signal was detected for half-reduced solutions of the quinone. An increase in pH from 9 to 12.5 resulted in an increase in EPR signal intensity. This observation is in accord with the comproportionation reaction of eq 6. Above pH 12.5 the intensity of the EPR signal decreased

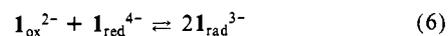


(Figure 3). This decrease in radical concentration can be shown

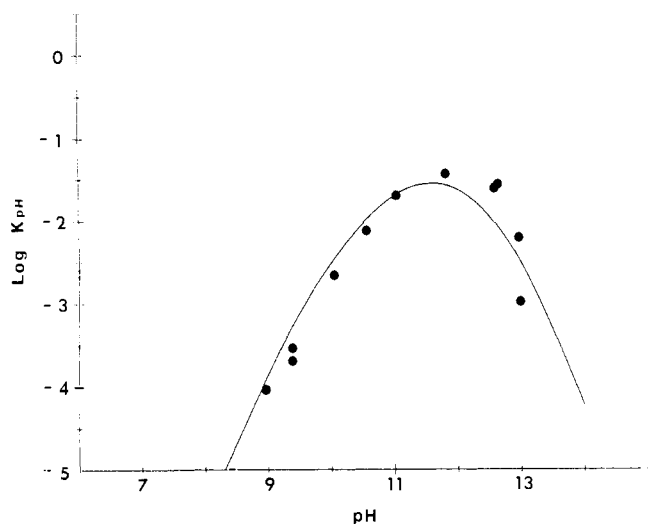


Figure 3. Changes in the log of the equilibria ($\log K_{pH}$) for comproportionation of I_{oxT} and I_{redT} as a function of pH. Experimental values of $\log K_{pH}$ (●) were determined by double integration of the EPR signals and the known concentration of I_{oxT} and I_{redT} . The theoretical curve was generated by eq 15 by utilizing constants from Table II (aqueous solution, $\mu = 0.1$).

Table I. Computed pH Dependence of $[I_{rad}^{3-}]$ on Comproportionation of Quinone and Quinol Both Initially at 1.3×10^{-4} M

pH	$[I_{radT}]$, μ M	pH	$[I_{radT}]$, μ M
8.99	1.27	11.85	22.86
9.41	1.89	12.51	25.28
9.41	2.30	12.60	19.12
10.07 ^a	6.03	12.67	20.16
10.57	11.04	12.98	9.89
11.06	17.24	13.01	4.26

^aDeuteriated buffer.

to be due to a decrease in quinone concentration which results from its pseudobase formation at high pH. The quinone hydrate cannot undergo comproportionation with I_{red}^{4-} to provide I_{rad}^{3-} . The determined concentrations of I_{rad}^{3-} as a function of pH are summarized in Table I.

The experimentally determined pH-dependent equilibrium constant for the comproportionation reaction may be written as shown in eq 7. The quantities I_{oxT} , I_{redT} , and I_{radT} are defined in eq 8–10. By material balance, when the various equilibrium

$$K_{eq} = \frac{[I_{radT}]^2}{[I_{oxT}][I_{redT}]} \quad (7)$$

$$I_{oxT} = (I_{ox}H_3^+ + I_{ox}H_2 + I_{ox}H^- + I_{ox}^{2-} + I_{ox}(OH)^{3-} + I_{ox}(H_3O_2)^{3-}) \quad (8)$$

$$I_{redT} = (I_{red}H_4 + I_{red}H_3^- + I_{red}H_2^{2-} + I_{red}H^{3-} + I_{red}^{4-}) \quad (9)$$

$$I_{radT} = (I_{rad}H^{2-} + I_{rad}^{3-}) \quad (10)$$

and acid dissociation constants and the definitions of eq 8–10 are employed, there is obtained eq 11–13. In eq 11–13 only equilibria involving pK_a values larger than 8 were considered because no

$$[I_{redT}] = [I_{red}H_2] \frac{a_H^2 + K'_3 a_H + K'_3 K'_4}{K'_3 K'_4} \quad (11)$$

$$[I_{radT}] = [I_{rad}H] \frac{K_{r1} + a_H}{K_{r1}} \quad (12)$$

$$[I_{oxT}] = [I_{ox}^{2-}] \frac{K_1 K_2 K_3 K_w + a_H K_w K_1 (1 + K_2) + a_H^2}{a_H^2} \quad (13)$$

EPR signal was detected below pH 9. In eq 13, K_3 represents

Table II. Comparison of Independently Determined (obsd) Equilibrium Constants to Those Employed (calcd) To Generate the Best Fit to the Experimental Points of Figure 3 by Use of Equation 15

	K_{calcd}	pK_{calcd}	pK_{obsd}
K	3.3		
K_{r1}	3×10^{-8}	7.52	
$K_w K_{sb}$	9×10^{-12}	11.05	10.73
K_3	5.5×10^{-13}	12.26	
K'_3	4.9×10^{-10}	9.31	9.31
K'_4	1.2×10^{-13}	12.92	12.94

Table III. ESR Hyperfine Coupling Constants for the 9-Decarboxymethoxatin Semiquinone

nucleus	a , G	position
N	0.60	unknown
N	0.81	unknown
H	1.02	1
H	1.26	unknown
H	0.80	9
H	1.84	unknown

the acid dissociation constant for the pyrrole N–H function. It was assumed that $K_1 K_2 \sim K_1 (1 + K_2)$ as the product of the latter is 1268 M^{-1} . Substituting eq 11–13 into eq 7 allows the derivation of eq 15 where the pH-independent constant K is defined by eq 14.

$$K = \frac{[I_{rad}^{2-}]}{[I_{ox}^{2-}][I_{red}H_2^{2-}]} \quad (14)$$

$$K_{pH} = K \left(\frac{K'_3 K'_4}{K_{r1}} \right) \times \left(\frac{a_H^2 (K_{r1}^2 + 2a_H K_{r1} + a_H^2)}{(K'_3 K'_4 + a_H K'_3 + a_H^2)(K_3 K_{sb} + a_H K_{sb} + a_H^2)} \right) \quad (15)$$

The constants employed with eq 15 to simulate the line fitting of the experimental points of Figure 3 are provided in Table II where they are compared to the experimentally determined constants. Inspection of Table II shows that the pK_a values used in eq 15 to obtain the best fit to the plot of $\log K_{pH}$ vs. pH agree within experimental error with those determined titrimetrically. From the fitting of the experimental $\log K_{pH}$ values, the value of the pH-independent comproportionation constant K (eq 14) is determined to be 3.3. The theoretical curves generated from eq 15 were found to fit the experimental points much better than did curves generated by deletion of the dissociation constant for the pyrrole proton of the oxidized form or by including a similar term for the reduced or semiquinone forms of 9-decarboxymethoxatin. When the hydration term was omitted from eq 15, the theoretical curve reached a maximum value around pH 12.5 and remained at this value.

Absorption spectra of half-reduced solutions at several pH values (Figure 4) were performed to determine the VIS spectrum of $I_{rad}^{2-} + I_{rad}^{3-}$. As seen in Figure 4B, the peak at 460 nm (pH 10.58) slowly decreases with time, while the 395-nm absorbance increases until they reach their "equilibrium" values. This behavior has also been observed for the semiquinones of other *o*-quinones (9,10-phenanthrenequinone and 9,10-acenaphthenequinone)¹⁴ by Staples and Szwarc who showed the spectral change to be due to conversion of the paramagnetic (red) radical anion to its (green) diamagnetic dimer. The peak at 395 nm (Figure 4) and the broad band between 500 and 800 nm may be due to dimerization of I_{rad}^{3-} . Such long-wavelength absorbance was reported for the radical dimers studied by Staples and Szwarc. Similarly, the peak at 460 nm can be ascribed to the paramagnetic monomer species. Because of this apparent interconversion of the paramagnetic and diamagnetic species and the possibility of the formation of higher

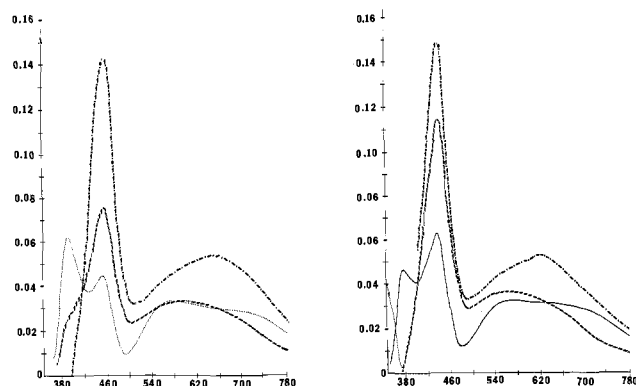


Figure 4. (A, right) UV/Visible spectra of I_{radT} obtained immediately after mixing solutions of quinone and quinol (each at 1.3×10^{-4} M). (B, left) Final spectrum after equilibration of paramagnetic monomer and diamagnetic dimer. The spectra of these species have each been determined at pH 10.58 carbonate buffer (●, B; —, A) pH 12.09 phosphate buffer (■ ■■), and pH 12.84 phosphate buffer (■ ■■).

aggregates, no attempt was made to determine extinction coefficients for the radical species. It has been reported that the radical anion is preferentially stabilized by the presence of Li^+ in THF solvent.¹⁵ At pH 12.20, the addition of Li^+ to 0.1 M was found to prevent the changes with time of the VIS spectrum of I_{rad}^{3-} which we have attributed to dimerization.

The influence of radical dimerization upon the pH profile for the comproportionation reaction (Figure 3) must be considered since the concentrations of radical species have been determined by EPR measurements and the diamagnetic dimeric species is EPR silent. The value of the equilibrium constant (K_{Dim}) for I_{rad}^{3-} dimerization (eq 16) is pH independent in the pH range of the

$$K_{Dim} = \frac{[I_{rad}^{3-}]_2}{[I_{rad}^{3-}]^2} \quad (16)$$

EPR measurements of Figure 3. This must be so, since the pK_a for ionization of I_{rad}^{2-} to I_{rad}^{3-} is below that of the lowest pH employed. Thus, the theoretical plot of Figure 3 possesses the correct shape but is displaced downward on the $\log K_{pH}$ axis. This displacement is equal to $\log K_{Dim}$ and cannot be large since by spectrophotometry it can be shown that both I_{rad}^{3-} and $(I_{rad}^{3-})_2$ are always present together.

EPR Spectral Analysis of I_{rad}^{3-} . The species I_{rad}^{3-} is a structural analogue of the semiquinone radical anion of the naturally occurring methoxatin coenzyme. It was of interest to compare the EPR spectral properties of I_{rad}^{3-} with that published by Westerling et al. for the radical anion of methoxatin.¹⁶ They measured the isotropic EPR spectrum of the methoxatin semiquinone in alkaline buffer containing high concentrations of salicylate. Their analysis resulted in the finding of two coupled nitrogens and three coupled protons. One of the coupled protons was observed to be exchangeable with deuterium if the spectrum was measured in D_2O .

As shown in Figure 5, the room-temperature EPR spectrum of half-reduced 9-decarboxymethoxatin at pH 10.47 is highly resolved with a total line width of 7.69 G which is 0.81 G greater than that of the methoxatin semiquinone. Thus, the 9H in I_{rad}^{3-} can be assigned with an $A_H = 0.81$ G. Calculation of the total line width (T.W.) of the I_{rad}^{3-} spectrum using eq 17¹⁷ and the

$$T.W. = 2 \sum_{i=1}^n n^i I^i a^i \quad (17)$$

isotropic coupling constants of Westerling et al. for the methoxatin semiquinone results in a value (7.7 G) similar to that observed experimentally (7.69 G) for I_{rad}^{3-} . Spectral simulations (Figures

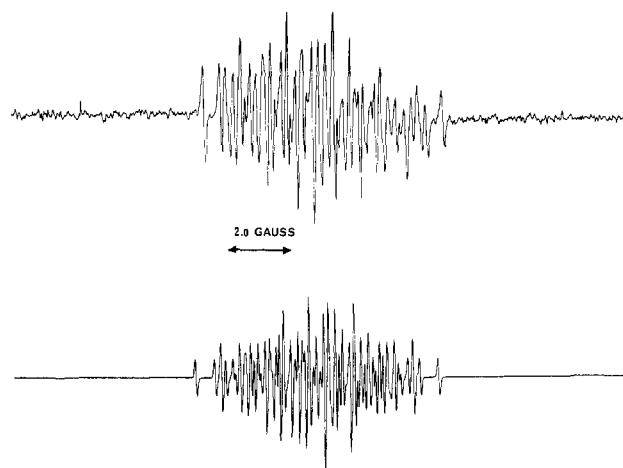


Figure 5. ESR spectrum of 9DCM semiquinone in H_2O . 9DCM (0.26 mM) in Na_2CO_3 buffer ($\mu = 0.1$), pH 10.47, was half-reduced with dithionite under an argon atmosphere: top, experimental spectrum; bottom, simulated spectrum using the nuclear hyperfine coupling constants given in Table III, a Gaussian line shape, and a line width of 0.1 G.

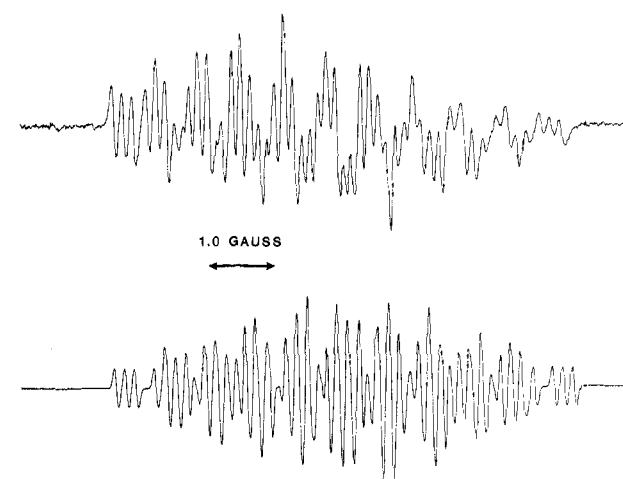


Figure 6. ESR spectrum of 9DCM semiquinone in D_2O : top, experimental spectrum; bottom, simulated spectrum using the nuclear hyperfine coupling constants given in Table III, with the exception that the proton with a coupling constant of 1.02 was assumed to exchange with deuterium and the deuterium nuclear properties were substituted in the simulation. Other conditions are as given in the caption of Figure 5.

5 and 6) using a Gaussian line shape show reasonable agreement with the experimental spectrum.

The EPR spectrum of I_{rad}^{3-} in D_2O (10.07 pD) exhibits a line width of 6.98 G which is a result of the replacement of a coupled proton with a deuteron (Figure 6). The exchangeable coupled proton is assigned to the proton on the N(1)-position with $A_H = 1.02$ G. This value is in good agreement with that found by Westerling et al.¹⁶ of 0.97 G for the exchangeable proton on methoxatin semiquinone. Simulation of the spectrum assuming one exchangeable proton (Figure 6) gives a reasonable fit of the experimental spectrum.

These data show there to be no major alterations in spin density in the heterocyclic trinuclear ring system on replacement of the 9-position carboxylate functionality in the naturally occurring coenzyme with a proton. It is of interest that ENDOR studies on quinoenzyme methanol dehydrogenase show an exchangeable coupled proton with a coupling constant of 1.03 G.¹⁸ Thus, by analogy with the model systems, the N(1)-position on the protein-bound methoxatin semiquinone exhibits a similar spin density. The EPR spectral data and simulations also suggest that the

(15) Maruyama, K. *Bull. Chem. Soc. Jpn.* **1964**, *37*, 553.

(16) Westerling, J.; Frank, J.; Duine, J. A. *Biochem. Biophys. Res. Commun.* **1979**, *87*, 710.

(17) Pederson, J. A. In *CRC Handbook of EPR Spectra from Quinones and Quinols*; CRC: Boca Raton, 1985; p 167.

(18) Duine, J. A.; Frank, J.; De Beer, R. *Arch. Biochem. Biophys.* **1984**, *233*, 708.

semiquinone form does not exist in a hydrated form as does the oxidized form. No reasonable simulations could be accomplished if one assumes hydration of $\mathbf{1}_{\text{rad}}^{3-}$.

It should be noted that in this study EPR spectra on semiquinone solutions above pH 12 exhibited less spectral resolution than those observed below pH 12. This is in contrast to the apparent high resolution of the spectrum of methoxatin semiquinone at pH 13 in 2 M salicylate.¹⁶ Thus, as in the presence of Li^+ (loc. cit.), the presence of salicylate may alter intermolecular interactions such as semiquinone self-aggregation or aggregation of semiquinone with oxidized or hydroquinone forms. In addition,

the presence of such agents probably also serves to alter the water structure. By means of a potentiometric titration, Duine et al.⁷ determined an equilibrium constant of 2.54 for the comproportionation of methoxatin at pH 13 in salicylate buffer. This value exceeds our value of K_{pH} at pH 13 with $\text{H}_2\text{O}/\text{HO}^-$ buffer (Table I) by almost 10^3 .

Acknowledgment. This work was supported by NIH grants to T.C.B. (AM 09171-22) and D.E.E. (GM-29433) and a graduate opportunity fellowship to E.J.R. provided by the University of California.

Supramolecular Catalysis in the Hydrolysis of ATP Facilitated by Macrocyclic Polyamines: Mechanistic Studies

Mir Wais Hosseini, Jean-Marie Lehn,* Linda Maggiora,[†] Kristin Bowman Mertes,[†] and Mathias P. Mertes*[†]

Contribution from the Institut Le Bel, Université Louis Pasteur, F-67000 Strasbourg, France, and the Departments of Chemistry and Medicinal Chemistry, University of Kansas, Lawrence, Kansas 66044. Received August 5, 1986

Abstract: Protonated polyaza macrocycles that bind anionic substrates can perform reactions on the bound species and provide information on the various factors contributing to catalysis. They form stable complexes with adenosine triphosphate, adenosine diphosphate, and pyrophosphate, and these supramolecular assemblies catalyze the solvolysis of the bound substrates. ³¹P NMR was found to be a useful technique both for the kinetic analysis and for the detection of unstable intermediates formed in the reaction. The 24-membered macrocyclic polyamine, 1,4,7,13,16,19-hexaaza-10,22-dioxocyclotetradecane ([24]N₆O₂, **1**), catalyzed the hydrolysis of ATP at both pH 3 and 7 with calculated entropies of activation of -11 and -8.7 eu. The reaction is insensitive to ionic strength; however, both sodium and chloride ions depress the k_{obsd} at pH 7. The reaction at neutral pH is characterized by nucleophilic catalysis with the formation of the symmetrical monophosphorylated derivative **2** of macrocycle **1**; a ΔS^* of -26 eu was found for the solvolysis of **2** at pH 7. A series of related 22- to 32-membered rings containing up to 10 groups demonstrated specific structural requirements for effective catalysis of the hydrolytic reactions. Analogues of **1** wherein the oxygen atoms are either replaced by amino groups ([24]N₈, **4**) or removed ([22]N₂C₄, **6**) enhanced the rate of ATP hydrolysis at pH 3 by a factor of 300. Clear evidence for electrostatic and nucleophilic catalysis coupled with potential sites for acid and base catalysis make such macrocycles fruitful materials for the study of the mechanisms of molecular catalysis in polyphosphate hydrolysis, as well as models for the processes that may occur in enzymes utilizing ATP and related species as substrates or phosphoryl donors.

The design of molecular catalysts may provide invaluable probes for the elucidation of the origin of the efficiency and selectivity in chemical and enzymatic catalytic processes.^{1,2} Supramolecular catalysis, catalysis within a supramolecular species, involves initial substrate binding by a receptor molecule bearing reactive groups, followed by transformation of the bound species and, thereafter, release of the products, so as to regenerate the catalyst for a new cycle.³

Mechanistic studies exploring the factors that determine the efficiency and selectivity of such catalysts are vital not only to the understanding of the elementary steps of catalytic processes but also to the future development of synthetic reagents designed for specific chemical reactions as well as to the elaboration of model systems capable of revealing factors that contribute to enzymatic catalysis.¹⁻⁴

Two such processes of contemporary interest are studies on phosphoryl group transfer from reactive anhydrides and phosphate ester formation and cleavage in polynucleotides. Prominent in the former group are reactions utilizing the principal biological energy store: adenosine triphosphate (ATP), a stable polyvalent anion at neutral pH that is the substrate for the highly efficient group of enzymes termed ATPases. Of particular interest are the factors that contribute to the 10^{10} -fold difference between the uncatalyzed and the ATPase-catalyzed hydrolysis of ATP.

In the search for catalytic effects extensive studies on the role of the biologically important divalent calcium, manganese, and magnesium cations have been reported.⁵ Cobalt(III)-amine complexes induce significant rate enhancements;⁶ however, studies with other metals have not found large catalytic effects. Naturally occurring acyclic polyamines putrescine, cadaverine, spermidine, and spermine bind nucleotides⁷ but are devoid of catalytic activity on ATP hydrolysis. An increase in the chain length of the

(1) Jencks, W. P. *Catalysis in Chemistry and Enzymology*; McGraw-Hill: New York, 1969.

(2) Walsh, C. F. *Enzymatic Reaction Mechanisms*; W. H. Freeman: San Francisco, 1979.

(3) (a) Lehn, J. M. *Science (Washington, D.C.)* **1985**, *227*, 849-856. (b) Lehn, J. M. *Pure Appl. Chem.* **1979**, *51*, 979-997. (c) Lehn, J. M. *Ann. N.Y. Acad. Sci.* **1986**, *471*, 41-50.

(4) (a) Breslow, R. *Science (Washington, D.C.)* **1982**, *218*, 532-537. (b) Kellogg, R. M. *Top. Curr. Chem.* **1982**, *101*, 111-145. (c) Tabushi, I.; Yamamura, K. *Top. Curr. Chem.* **1983**, *113*, 145. (d) Murakami, Y. *Top. Curr. Chem.* **1983**, *115*, 107-155. (e) Sirlin, C. *Bull. Soc. Chim. Fr.* **1984**, 15-40.

(5) (a) Tetas, M.; Lowenstein, J. M. *Biochemistry* **1963**, *3*, 350-357. (b) Taqui Khan, M. M.; Martell, A. E. *J. Am. Chem. Soc.* **1967**, *89*, 5385-5390. (c) Frey, C. M.; Banyasz, J. L.; Stuehr, J. E. *J. Am. Chem. Soc.* **1972**, *96*, 9298-9204.

(6) (a) Suzuki, S.; Higashiyama, T.; Nakahara, A. *Bioinorg. Chem.* **1978**, *8*, 277-289. (b) Hediger, M.; Milburn, R. M. *J. Inorg. Biochem.* **1982**, *16*, 165-182. (c) Milburn, R. M.; Gatum-Basak, M.; Tribolet, R. J.; Sigel, H. *J. Am. Chem. Soc.* **1985**, *107*, 3315-3321 and references therein.

(7) Nakai, C.; Glinsmann, W. *Biochemistry* **1977**, *16*, 5636-5641.

*Department of Medicinal Chemistry, University of Kansas.

[†]Department of Chemistry, University of Kansas.